Received: 25 December 2021 | Revised: 22 April 2022 | Accepted: 10 May 2022

DOI: 10.1096/fj.202101977RR

RESEARCH ARTICLE

THE FASEB JOURNAL

HDM induce airway epithelial cell ferroptosis and promote inflammation by activating ferritinophagy in asthma

Zhaojin Zeng[1] | Haohua Huang[1] | Jinming Zhang[1] | Yuanyuan Liu[1] | Wenshan Zhong[1] | Weimou Chen[1] | Ye Lu[1] | Yujie Qiao[1] | Haijin Zhao[1] | Xiaojing Meng[2] | Fei Zou[2] | Shaoxi Cai[1] | Hangming Dong[1]

[1]Chronic Airways Diseases Laboratory, Department of Respiratory and Critical Care Medicine, Nanfang Hospital, Southern Medical University, Guangzhou, China

[2]Guangdong Provincial Key Laboratory of Tropical Disease Research, Department of Occupational Health and Medicine, School of Public Health, Southern Medical University, Guangzhou, China

Correspondence
Shaoxi Cai and Hangming Dong, Chronic Airways Diseases Laboratory, Department of Respiratory and Critical Care Medicine, Nanfang Hospital, Southern Medical University, Guangzhou, China.
Emails: hxkc@smu.edu.cn and dhm@smu.edu.cn

Funding information
National Natural Science Foundation of China, Grant/Award Number: 81870058, 81970032 and 82170032; Natural Science Foundation of Guangdong Province, Grant/Award Number: 2017A030313849

Abstract

Asthma is a disease characterized by airway epithelial barrier destruction, chronic airway inflammation, and airway remodeling. Repeated damage to airway epithelial cells by allergens in the environment plays an important role in the pathophysiology of asthma. Ferroptosis is a novel form of regulated cell death mediated by lipid peroxidation in association with free iron-mediated Fenton reactions. In this study, we explored the contribution of ferroptosis to house dust mite (HDM)-induced asthma models. Our in vivo and in vitro models showed labile iron accumulation and enhanced lipid peroxidation with concomitant nonapoptotic cell death upon HDM exposure. Treatment with ferroptosis inhibitors deferoxamine (DFO) and ferrostatin-1 (Fer-1) illuminated the role of ferroptosis and related damage-associated molecular patterns in HDM-treated airway epithelial cells. Furthermore, DFO and Fer-1 reduced HDM-induced airway inflammation in model mice. Mechanistically, NCOA4-mediated ferritin-selective autophagy (ferritinophagy) was initiated during ferritin degradation in response to HDM exposure. Together, these data suggest that ferroptosis plays an important role in HDM-induced asthma and that ferroptosis may be a potential treatment target for HDM-induced asthma.

KEYWORDS

asthma, autophagy, ferroptosis, inflammation, iron, oxidative stress

1 | INTRODUCTION

Asthma is a chronic airway disease that is characterized by inflammation, shedding of airway epithelial cells, and airway remodeling.[1] Allergic asthma, the most common form of asthma, can be triggered by allergens, such as house dust mites (HDM).[2] As the first defensive barrier between the lungs and external environment, airway

Abbreviations: 4HNE, 4-hydroxynonenal; COPD, chronic obstructive pulmonary disease; CQ, chloroquine; DAMPs, release damage-associated molecular patterns; DFO, deferoxamine; FASH, ferrous ammonium sulfate hexahydrate; Fer-1, ferrostatin-1; FTH, ferritin heavy chain; GPX4, glutathione peroxidase 4; HDM, house dust mite; HO-1, heme oxygenase 1; NCOA4, nuclear receptor coactivator 4; Nec-1, necrostatin-1; Nrf2, nuclear factor erythroid2-related factor 2; ROS, reactive oxygen species; TDI, toluene diisocyanate; TFR, transferrin receptor.

This is an open access article under the terms of the Creative Commons Attribution-NonCommercial-NoDerivs License, which permits use and distribution in any medium, provided the original work is properly cited, the use is non-commercial and no modifications or adaptations are made.
© 2022 The Authors. *The FASEB Journal* published by Wiley Periodicals LLC on behalf of Federation of American Societies for Experimental Biology

epithelial cells play important roles in defense, antigen presentation, and the quick response to different allergens.[3] Epithelial damage is a pathological feature observed in all asthma phenotypes.[4] Moreover, damaged airway epithelium attracts inflammatory cells by releasing cytokines and chemokines,[5] and the recruited cells contribute to airway hyperresponsiveness.[6] Hence, it is essential to understand the mechanisms of epithelial damage in response to various allergens.

Ferroptosis, a novel form of nonapoptotic cell death, is characterized by the accumulation of reactive oxygen species (ROS) derived from iron metabolism and lipid peroxidation,[7] and dying cells can release damage-associated molecular patterns (DAMPs), which have been linked to an enhanced inflammatory response and tissue damage.[8] The lipid repair enzyme glutathione peroxidase 4 (GPx4), a member of the selenoprotein family, has been shown to act as a negative regulator of ferroptosis by directly reducing lipid hydroxyperoxidation.[9,10] Ferroptosis was initially observed in cancer cells expressing oncogenic RAS, but it may contribute to other diseases, such as Huntington disease and tubular failure.[11] Recent studies have implicated ferroptosis in intestinal diseases, including intestinal ischemia/reperfusion injury, inflammatory bowel disease, and colorectal cancer.[12–15] In various acute kidney injury models, ferroptotic processes were observed and/or inhibited by ferroptosis inhibitors, such as ferrostatin-1 and liproxstatin-1, to confer renal protection.[16–18] Ferroptosis has been observed in acute lung injury, pulmonary fibrosis, and chronic obstructive pulmonary disease (COPD).[19–21] Recent studies on asthma have confirmed that the small scaffolding protein PEBP1 regulates ferroptotic cell death by binding with lipoxygenases, allowing them to generate lipid peroxides in asthmatic airway epithelial cells.[22,23]

Oxidative stress, specifically that caused by lipid peroxidation, is believed to contribute to the pathophysiology of asthma.[24,25] The lung iron level plays a crucial role in the pathogenesis and severity of asthma.[26] Moreover, Zn/Ga-deferoxamine (DFO), a ferroptosis inhibitor that tightly binds redox active metals such as iron and prevents their participation in the ROS-producing Fenton reaction, attenuating the inflammatory process in a mouse model of asthma.[27] Intracellular iron is stored primarily as ferritin, yet free iron is required for oxidative modifications during Fenton reactions. Thus, disruption of iron homeostasis can increase oxidative stress and tissue damage in asthma. Recent reports have revealed that labile iron is produced by autophagy-related ferritin degradation in a process termed ferritinophagy, and this newly discovered form of autophagy depends on a selective cargo receptor, nuclear receptor coactivator 4 (NCOA4), that traffics ferritin to the autophagosome.[28] Interestingly, ferritinophagy has been reported to be involved in ferroptosis.[29] In this study, we found that HDM induce NCOA4-mediated ferritinophagy, resulting in an increase in free iron in airway epithelial cells and promoting inflammation.

Taken together, our findings revealed that HDM promote labile iron accumulation via NCOA4-mediated ferritinophagy, leading to ferroptosis of airway epithelial cells, suggesting ferroptosis as a therapeutic target for asthma treatment.

2 | MATERIALS AND METHODS

2.1 | Reagents and antibodies

The antibodies used were mouse anti-Ferritin Heavy Chain (Santa Cruz, sc-376594), rabbit anti-Ferritin Heavy Chain (Cell Signaling Technology, 4393), mouse anti-NCOA4 (Santa Cruz, 373739), rabbit anti-NCOA4 (Affinity, DF4255), rabbit anti-ATG5 (Cell Signaling Technology, 12994), rabbit anti-GPx4 (Abcam, 125066), rabbit anti-GPx4 (Proteintech, 14432) mouse anti-4-HNE (Abcam, ab48506), rabbit anti-HO-1 (Affinity, AF5393), rabbit anti-Nrf2 (Proteintech, 16396), rabbit anti-Transferrin receptor (Abcam, ab214039),and mouse anti-β-actin (Proteintech, 66009). Antibody dilutions were according to manufacturer's instructions.

The following reagents were used: Deferoxamine (Sigma-Aldrich, D9533), Ferrostatin-1 (Medchemexpress, HY-100579), Necrostatin-1 (Medchemexpress, HY-15760), Z-VAD-FMK (Medchemexpress, HY-16658B), CQ (Medchemexpress, HY-17589A).

2.2 | Cell culture

Bronchial epithelial cell line HBE135-E6E7 (ATCC, CRL-2741) was cultured in KM (Sciencell, 2101) in 5% CO_2 and 95% humidity at 37°C.

2.3 | Animal and experiment design

BALB/c mice (female, 6-week old, 20–24 g) were purchased from Guangdong Medical Laboratory Animal Center. The mice were housed in the laboratory with a 12:12-h light/dark cycle at 24°C in an atmosphere of 40%–70% humidity. Food and water were sterilized and all experiments involving animals complied with the ARRIVE guidelines. All the animal experiments were approved by the Committee on the Ethics of Animal Experiments of Southern Medical University in Guangzhou, China and performed under standard guidelines for the Care and Use of Laboratory Animals. HDM was purchased from ALK-Abello A/S.

Thirty-two BALB/c mice were randomly distributed to four groups: (1) control group, (2) HDM group, (3) HDM+DFO group, and (4) HDM + ferrostatin-1 (Fer-1) group. Mice were challenged by intraperitoneal injection of 0.2 ml of saline solution containing HDM (400 U) on day 0 and day 7. Then, the mice were challenged intranasally every other day during 3 weeks, with 0.02 ml of saline solution containing HDM (400 U) or saline as control. Inhibitor of ferroptosis, DFO (100 mg/kg) and Fer-1 (20 mg/kg), was administered intraperitoneally 1 h before each HDM challenge. All the mice were sacrificed on day 28.

2.4 | Cell viability and Cell death assay

For the assessment of cell viability, HBE cells were treated with the Cell Counting Kit-8 reagent (Dojindo, CK04) according to the manufacturer's instructions. For the assessment of cell death, HBE cells were seeded in 12-well culture plates and treated with Viability/Cytotoxicity Assay Kit (Proteintech, PF00007). Cells were rinsed in PBS three times and incubated for 20 min in the dark at room temperature in 2 μmol/L Calcein-AM and 5 μmol/L PI. Under blue light excitation, living cells appeared green fluorescence and the nuclei of dead cells displayed red fluorescence (per Calcein-AM, PI instructions).

2.5 | Measurement of lipid peroxidation in vitro

HBE cells were seeded in 15 mm glass bottom cell culture dish and treated as described above. Lipid peroxidation was measured using a C11-BODIPY 581/591 probe (Ther moFisher Scientific, D3861). Briefly, cells were incubated for 30 min with C11 BODIPY 581/591 (1 μM) in growth medium. Fluorescence of C11 BODIPY was measured by simultaneous acquisition of the green (484/510 nm) and red signals (581/610 nm), providing a ratiometric indication of lipid peroxidation.

2.6 | Transmission electron microscopy

HBE cells treated with HDM or erastin were fixed with 2.5% glutaraldehyde fixator at room temperature and avoid light for 30 min, and then transferred to 4°C for storage. Photographed using transmission electron microscopy (TEM, HITACHI HT7700 120 kV).

2.7 | Measurement of MDA

Levels of MDA were determined with the MDA Assay Kit (Beyotime, S0131S) according to the manufacturer's instructions.

2.8 | Analysis of bronchoalveolar lavage fluid

Bronchoalveolar lavage fluid (BALF) samples were collected by flushing the right lungs three times with 1 ml PBS using a 1-ml syringe inserted into a cannula. Total cells in BALF were counted, and a cytospin sample was prepared and stained with Giemsa for blinded assessment of eosinophil cells percentages in BALF. Then BALF samples were centrifuged (1000 rpm, 10 min). The supernatants were harvested and stored at −80°C. The levels of IL-4, IL-5, IL-13, TNF-α, and IL-33 in the processed BALF samples were measured using Magnetic Luminex Assay (L141459) according to the manufacturer's instructions. In addition, the levels of HMGB1 (CUSABIO, E08225m) in BALF were measured using ELISA according to the manufacturer's instructions.

2.9 | Cytokines in cell

After the indicated treatment, the cell culture supernatant was collected and cell were lysed. Secretions of TNF-α (CUSABIO, E04740h) and intracellular levels of HMGB1 (CUSABIO, E08223h) and IL-33 (MEIMIAN, 8648) were measured using commercial ELISA kits according to the manufacturer's instructions.

2.10 | Transfection of siRNA and plasmids

Short interfering RNAs (siRNAs) were synthesized by GenePharma, and plasmids were synthesized by Hanbio. HBE cells transfections were conducted using Lipo3000 (Thermo Fisher Scientific) following the manufacturer's protocol. After 48 h, cells were further stimulated with different reagents. The successfully transfected clones were confirmed by western blotting. The following sequences were used in this study: GPX4 (sense, 5′-GACCGAAGUAAACUACACUTT-3′; antisense, 5′-AGUGUAGUUUACUUCGGUCTT-3′); NCOA4 (sense, 5′-GCAUAAAGAUUCCCUGAAUTT-3′; antisense, 5′-AUUCAGGGAAUCUUUAUGCTT-3′); ATG5 (sense, 5′-GACCUUUCAUUCAGAAGCUTT-3′; antisense, 5′-AGCUUCUGAAUGAAAGGUCTT-3′).

2.11 | Western blotting and co-immunoprecipitation

Total cell lysates were obtained using the Total Protein Extraction Kit (KeyGen Biotech) according to the manufacturer's instructions. Proteins were subjected to SDS-PAGE, transferred to PVDF membranes, and probed with various primary antibodies and LICOR: fluorescence-labeled secondary antibodies (#926-68071, 926-32210). Blots were visualized using a LICOR Odyssey fluorescent imaging system (LICOR Biotechnology) finally. For coimmunoprecipitation, protein extracts from cells were incubated with indicated primary antibody overnight at 4°C. The immune-complexes were cleared with Protein A/G Magnetic Beads (Thermo Scientific). Input lysates were run simultaneously with the IP samples on 10% polyacrylamidegels and visualized with LICOR Odyssey Scanner.

2.12 | Pathological staining and immunohistochemistry

Lung sections were stained with hematoxylin and eosin (H&E) to evaluate the degree of inflammatory cell infiltration around the bronchus. The expressions of GPX4, FTH, 4HNE, NCOA4, HO-1, and Nrf2 were characterized by immunohistochemistry using specific antibodies. Briefly, lung slices were dewaxed in xylene, followed by antigen retrieval with citrate buffer (pH 6.0) and incubated overnight with antibodies against GPX4 (Proteintech, 1:100), FTH (ABclonal, 1:100), 4HNE (Abcam, 1:100), NCOA4 (Affinity, 1:100), HO-1 (Affinity, 1:100) and Nrf2 (Proteintech, 1:100). Then, lung slices were incubated with secondary antibody for 30 min and visualized with a DAB substrate kit (Zhong Shan Jin Qiao).

2.13 | Iron assay

The level of iron in lung tissue was measured by Iron Assay Kit (Dojindo, I291) according to the manufacturer's instructions. And the level of iron in HBE cells were measured by Iron Colorimetric Assay Kit (Applygen, E1042) according to the manufacturer's instructions.

2.14 | Catalytic Fe (II) imaging

HBE Cells were seeded on a confocal dish for 24 h. After treatment, cells were washed three times with HBSS. Then, cells were incubated for 30 min at 37°C, 5% CO_2 incubator with RhoNox (Dojindo, F374) and LysoTracker Green DND-26 (Meilunbio, MB6042). The cells were imaged using the confocal microscope (Olympus Corporation).

2.15 | Flow cytometric analysis

HBE cells were seeded at a density of 2.5×10^5 cells per well in 6-well plates, and treated 24 h with or without HDM. The percentage of cells undergoing apoptosis was measured using flow cytometry with PI and Annexin-V double staining.

2.16 | Statistical analysis

Statistical analysis was performed by the GraphPad Prism 7 software (GraphPad). The *t* test was used to analyze differences between two groups, and one-way ANOVA was used to evaluate the statistical significance among groups. The results are presented as the mean ± standard deviation (SD) or mean ± standard error of mean (SEM), and values of $p < .05$ were considered statistically significant. At least three independent experiments were carried out for the statistical comparisons.

3 | RESULTS

3.1 | House dust mite (HDM) induce the ferroptosis of human bronchial epithelial cells

To elucidate the involvement of ferroptosis in HDM-mediated cell death, HDM-induced lipid peroxidation was evaluated by C11 BODIPY staining after 24 h of HBE cell exposure to HDMs. C11 BODIPY staining showed obvious lipid peroxidation in response to HDM exposure. DFO and Fer-1, two specific ferroptosis inhibitors, clearly abrogated HDM-induced lipid peroxidation (Figure 1A,B) and significantly inhibited HDM-induced cell death, as measured by Cell Counting Kit-8 (CCK-8) and viability/cytotoxicity assays, respectively (Figure 1D–F). DFO and Fer-1 also decreased the level of MDA (a lipid peroxidation product) in cells treated with HDM (Figure 1C). Western blot analysis results showed that both HDM and Erastin (a ferroptosis inducer) inhibited GPX4 protein expression (Figure 1G and Figure S1A). Ferroptosis as the mechanism of HDM-induced cell death was further supported by the flow cytometry results and the negligible effects of treatment with the necroptosis inhibitor necrostatin-1 (Nec-1) and the apoptosis inhibitor zVAD-FMK on HDM-induced cell death (Figure S1B,C).

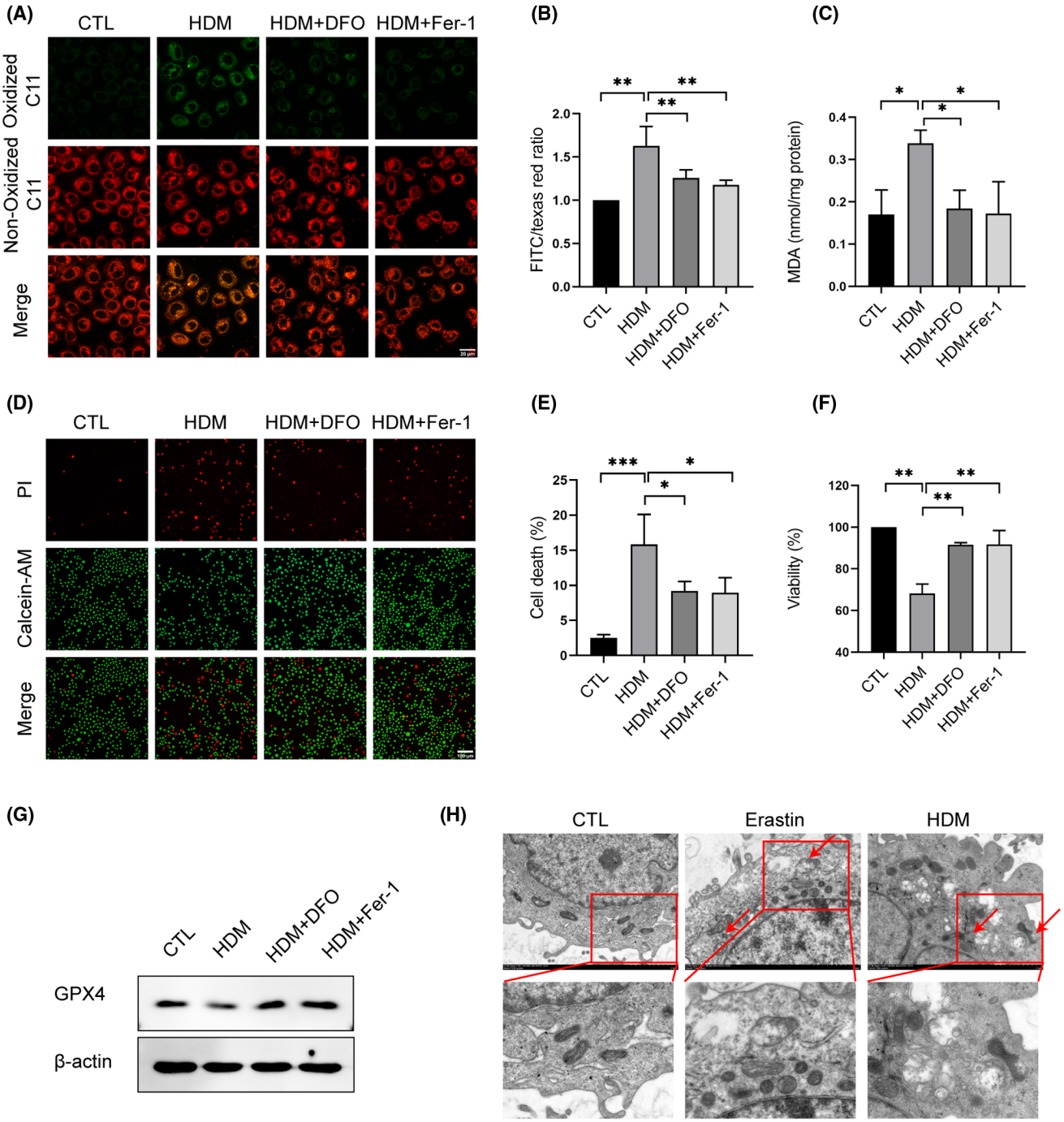

FIGURE 1 HBE cells were treated with house dust mite (HDM) (800 μ/ml) for 24 h. deferoxamine (50 μM) or ferrostatin-1 (20 μM) was added to HBE cells 1 h before HDM treatment. (A,B) Lipid peroxidation was assessed by C11 BODIPY staining, and quantitative analysis of fluorescence intensity of each group ($n = 4$). Scale bar = 20 μm. (C) Levels of MDA were determined by MDA Assay Kit. (D,E) Cell death was assessed by PI and Calcein-AM staining, and statistical analysis of death rates respectively of each group. Scale bar = 100 μm. (F) Cell viability was assessed by CCK8 assay. (G) Western blots analysis of GPX4 in cells from these four groups. (H) Representative images of mitochondrial injury at 24 h under indicated treatment were observed by TEM. Red arrow indicates damaged mitochondria. Scale bar = 2 μm. The data are presented as the mean ± SD, analyzed by one-way ANOVA with Dunnett's multiple comparison test. *$p < .05$, **$p < .01$.

As ferroptosis has unique morphological characteristics, we used transmission electron microscopy to monitor morphological changes caused by HDM. HBE cells exposed to HDM exhibited shrunken and damaged mitochondria, features unique to ferroptosis, with no other changes observed prior to cell death (Figure 1H).

Next, siRNA-mediated knockdown of GPx4, an intrinsic negative regulator of ferroptosis, was performed, and

efficient knockdown was confirmed by western blotting (Figure 2A). GPx4 knockdown significantly enhanced HDM-induced lipid peroxidation and death of HBE cells (Figure 2B–F). These data suggest that ferroptosis was the predominant form of HDM-induced cell death under our experimental conditions.

3.2 | Ferroptosis is involved in HDM-induced asthma in model mice

To evaluate the involvement of ferroptosis in airway epithelial cells in vivo, an asthma model was induced with BALB/c mice exposed to HDMs. Airway epithelial cell death in this in vivo model was evaluated through TUNEL assay (Figure 3A). TUNEL-positive cells were increased in HDM-exposed mouse lungs, while Fer-1 and DFO remarkably reduced the cell death rate (Figure 3B). Furthermore, the GPX4 protein was detected by western blot analysis. We found that the protein expression of GPX4 was decreased in mice exposed to HDM mice, and Fer-1 and DFO treatment mitigated the loss of GPX4 (Figure 3C). Immunohistochemistry showed similar results with mouse airway epithelial cells (Figure 3D). These data suggest that ferroptosis plays an essential role in the HDM-induced mouse asthma model.

3.3 | Inhibition of ferroptosis reduces HDM-induced airway inflammation

Imbalance in Th1/Th2 immunoregulation is a vital characteristic in asthma, in addition to airway inflammation. Next, we directed our study toward airway inflammation in asthmatic mice. Compared to HDM-induced mouse models, significantly decreased infiltration of

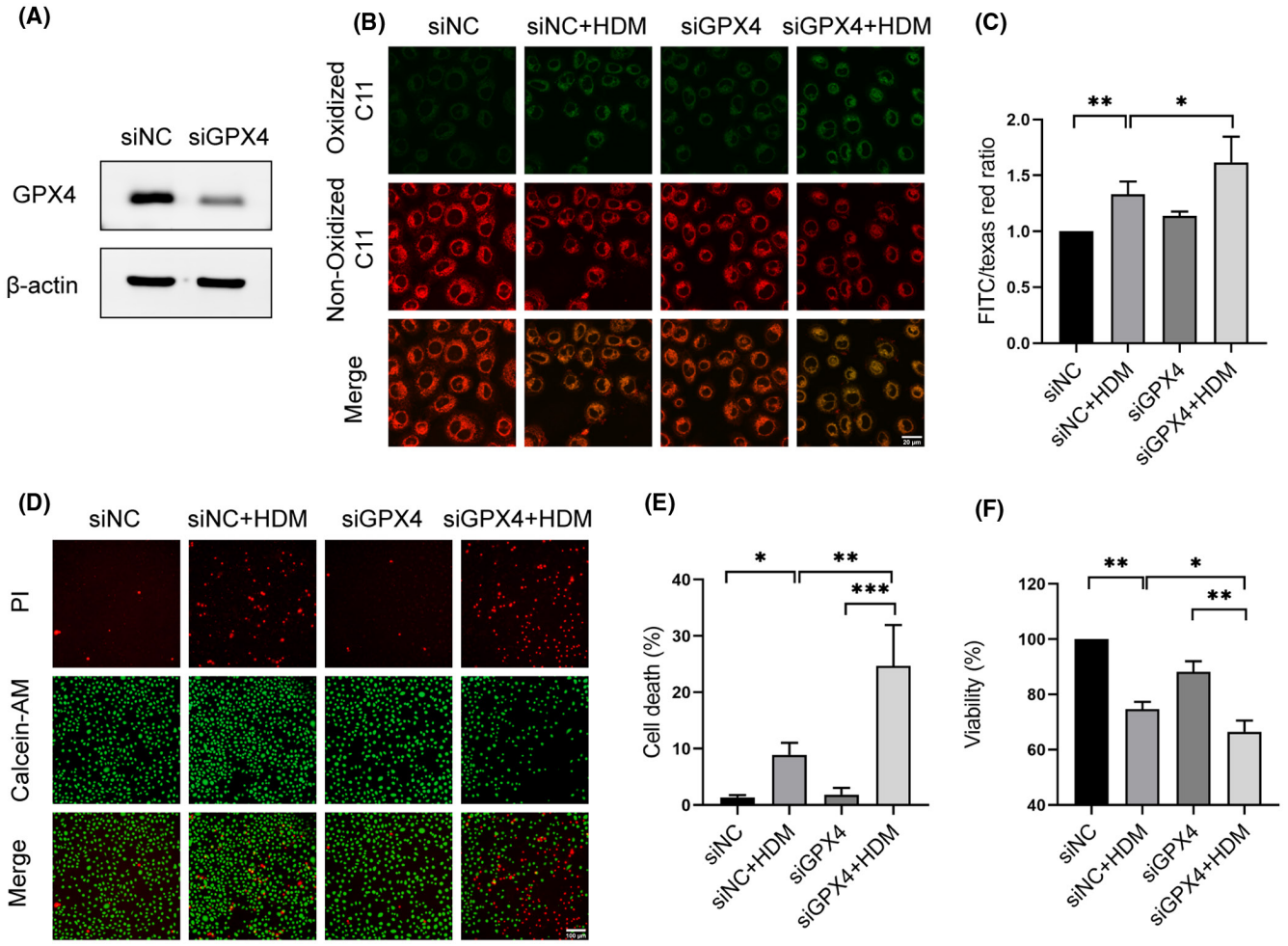

FIGURE 2 (A) Western blot showed the expression levels of glutathione peroxidase 4 (GPx4) in HBE cells transfected with control short interfering RNA (siRNA) or GPx4 siRNA. (B,C) Lipid peroxidation was assessed by C11 BODIPY staining, and quantitative analysis of fluorescence intensity of each group ($n = 4$). Scale bar = 20 μm. (D,E) Cell death was assessed by PI and Calcein-AM staining, and statistical analysis of death rates respectively of each group. Scale bar = 100 μm. (F) Cell viability was assessed by CCK8 assay. The data are presented as the mean ± SD, analyzed by one-way ANOVA with Dunnett's multiple comparison test. *$p < .05$, **$p < .01$. $n = 3$.

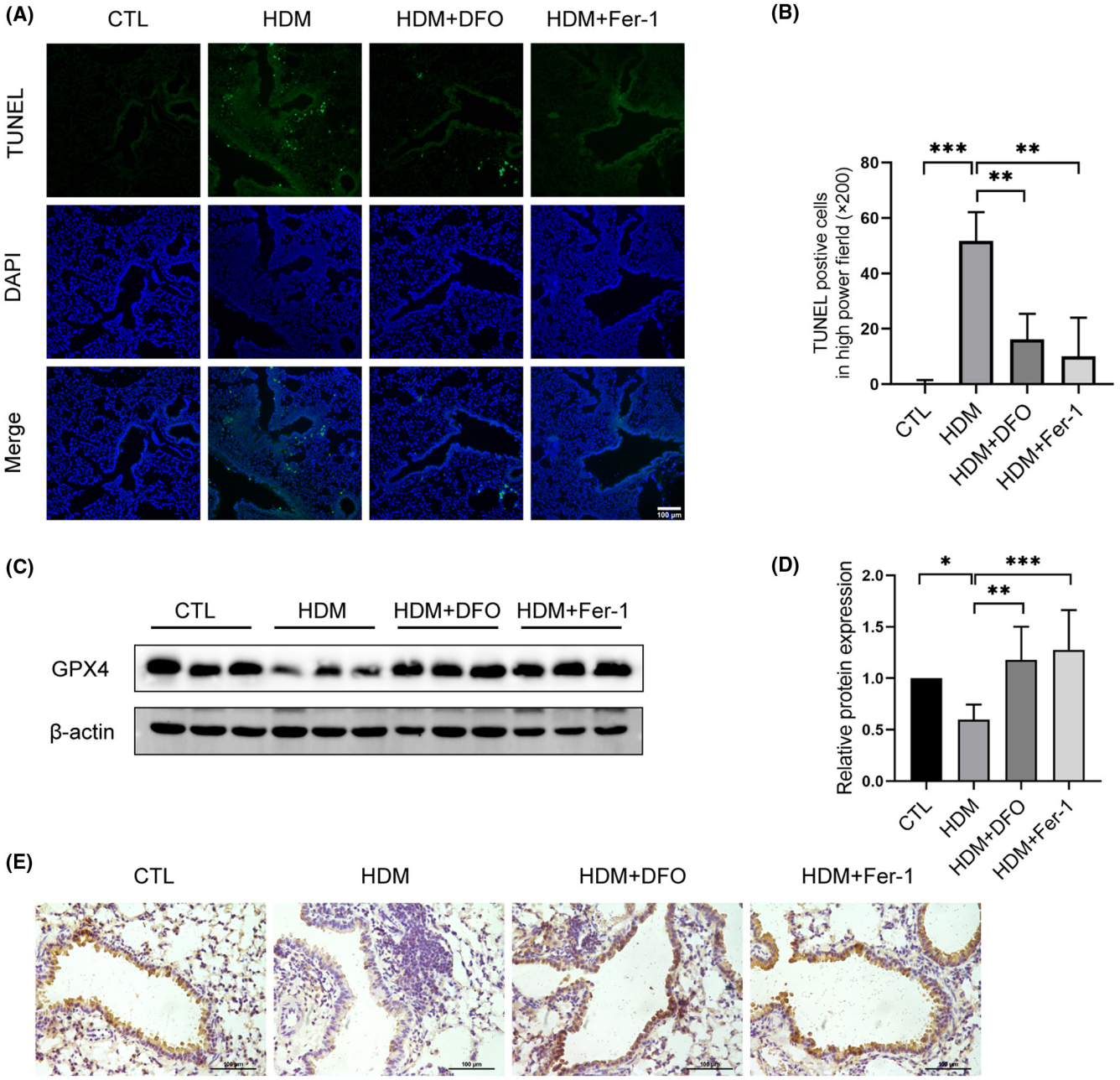

FIGURE 3 (A,B) TUNEL fluorescence staining and statistical analysis of cell death in mice lung sections. Green fluorescence in pictures represent positive signals (cell death), while blue fluorescence represent nuclear staining ($n \geq 4$). Scale bar = 100 μm. (C,D) Western blots analysis of GPX4 in lung tissue from these four groups and quantification of GPX4 protein levels relative to β-actin is shown ($n = 6$). (E) Immunohistochemical staining of GPX4 in mouse lung airway. The data are presented as the mean ± SD, analyzed by one-way ANOVA with Dunnett's multiple comparison test. *$p < .05$, **$p < .01$, ***$p < .001$.

total bronchoalveolar lavage fluid (BALF) cells and eosinophils was observed in the mice treated with Fer-1 and DFO (Figure 4B,C). H&E staining further revealed that the accumulation of airway inflammatory cells in the peribronchiolar and perivascular regions was clearly reduced in HDM-treated mice (Figure 4A). HDM stimulation led to increased levels of IL-4, IL-5 and IL-13 expression in the BALF cells of asthmatic mice, and this response was blocked by coadministration of Fer-1 or DFO (Figure 4D–F). The expression of TNF-α, IL-33 and HMGB1, known as proinflammatory molecules associated with ferroptosis, was increased in the BALF of HDM-induced mice, and the increase in these cytokines was attenuated by treatment with Fer-1 or DFO (Figure 4G–I). Furthermore, we got similar results in cell experiments (Figure 4J–L). These data indicate that DFO and Fer-1 reduced HDM-induced airway inflammation.

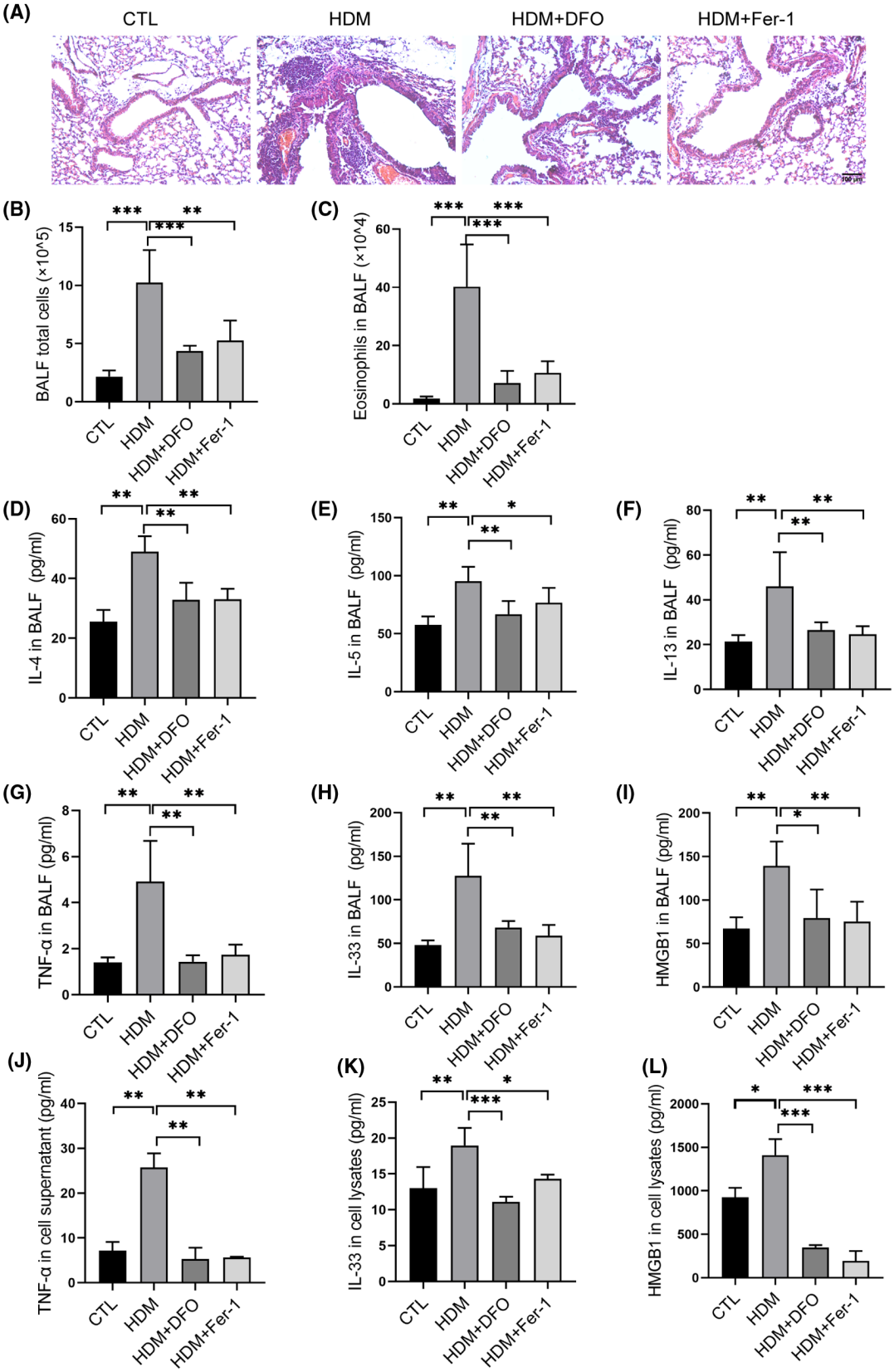

FIGURE 4 (A) Representative lung tissue sections stained with H&E. Scale bar = 100 μm. (B) Total bronchoalveolar lavage fluid (BALF) cell counts. (C) BALF eosinophil counts. (D–I) levels of IL-4, IL-5, IL-13, TNF-α, IL-33, HMGB1 in BALF ($n \geq 5$). (J) ELISA analysis of TNF-α levels in the cell culture supernatant from these four groups ($n = 3$). (K,L) ELISA analysis of IL-33 and HMGB1 levels in the cell lysates of HBE cells from these four groups ($n = 3$). The data are presented as the mean ± SD, analyzed by one-way ANOVA with Dunnett's multiple comparison test. *$p < .05$, **$p < .01$, ***$p < .001$.

3.4 | HDM induce increased free iron levels and promote oxidative stress

Increased free iron plays a critical role in Fenton reactions during ferroptosis. Next, we assessed whether HDM increase intracellular labile iron in experimental mouse models of asthma. The western blot analysis revealed that HDM exposure induced an increase in ferritin heavy chain (FTH) and transferrin receptor (TFR) expression in lung tissue (Figure 5B). And the iron assay results showed significantly higher concentration of iron in lung homogenates from HDM-exposed lungs, and DFO reduced the iron ion content, but Fer-1 had no effect (Figure 5A). The expression of FTH in lung tissue as detected by western blot analysis also indirectly reflected this increase in iron concentration (Figure 5C). Immunohistochemistry revealed the presence of FTH in epithelial cells, with increased signaling in the HDM-induced lungs of asthmatic mice, and this increase was abrogated by DFO (Figure 5D). Furthermore, immunohistochemical staining of the lipid peroxidation marker 4-hydroxynonenal (4HNE) showed that HDM greatly increased the production of 4-hydroxynonenal, particularly in airway epithelial cells, indicating aberrant lipid peroxidation during HDM-induced asthma. Moreover, Fer-1 or DFO pretreatment significantly decreased the expression of 4HNE (Figure 5D).

Our in vitro experiments also demonstrated that free iron levels in HBE cells were elevated after HDM exposure for 24 h (Figure 6A). In addition, we detected the protein levels of FTH, Nrf2 and HO-1 by western blotting and found a time-dependent increase in these proteins upon HDM stimulation (Figure 6B). Next, our western blot data showed that DFO decreased the expression of FTH, Nrf2, and HO-1, which had been increased by HDM exposure (Figure 6C). Similar to the results of our in vivo experiment, Fer-1 showed no obvious effect on the expression of FTH and increased Nrf2 and HO-1 expression. And we got similar results in cells treated with Erastin (Figure S2A,B). These results may have been results of Fer-1 increasing the antioxidant capacity of cells by increasing the expression of proteins such as Nrf2 and HO-1.

We verified that the increased iron level caused oxidative stress in HBE cells. We used ferrous ammonium sulfate hexahydrate (FASH) to stimulate the cells and measured intracellular iron levels 24 h later (Figure 6D). DFO significantly inhibited cell death induced by FASH (Figure 6G). C11 BODIPY staining showed that DFO clearly abrogated FASH-induced lipid peroxidation (Figure 6H,I). Next, we detected the protein levels of FTH, Nrf2 and HO-1 by western blot analysis, and all the western blot data showed similar results to those obtained after HDM exposure (Figure 6E,F). These results suggest that HDM aggravates oxidative stress by inducing an increase in free iron levels.

3.5 | Ferritinophagy is involved in HDM-induced cell death

Finally, we focused on how HDM cause an increase in intracellular iron levels. It has been previously demonstrated that the autophagic degradation of ferritin can promote ferroptosis and that NCOA4 is a selective cargo receptor that mediates ferritin degradation in lysosomes.[28] In this study, we investigated whether the NCOA4-mediated degradation of ferritin is associated with HDM-induced ferroptosis of epithelial cells. The western blot analysis and immunohistochemistry of mouse lung tissue revealed that HDM exposure induced an increase in NCOA4 expression in airway epithelial cells (Figure 7A,B). A coimmunoprecipitation analysis also showed that HDM caused an increase in the amount of FTH bound to NCOA4 (Figure 7C). Furthermore, NCOA4 knockdown inhibited HDM-induced ferritin degradation in HBE cells (Figure 7D). Additionally, we found that NCOA4 knockdown alleviated HDM-induced free iron level increases and reduced the cell death rate (Figure 7E,F). A recent study demonstrated that HDM activated autophagy in airway epithelial cells.[30] In agreement with this observation, HDM exposure increased the expression of the autophagy-related protein LC3 in HBE cells (Figure 7G). FTH accumulation was also enhanced when autophagy was inhibited by ATG5 and P62 siRNA transfection and by treatment with the autophagy inhibitor chloroquine (CQ) (Figure 7H,M and Figure S3B). ATG5 knockdown alleviated HDM-induced free iron level upregulation and cell death (Figure 7I,J). And we found that the co-localization of the ferrous (Fe^{2+}) iron and lysosomes increased significantly after HDM treatment by fluorescent probes (Figure 7K,L). To test whether there was a simultaneous degradation of FTH protein upon ferroptosis induction, we transfected plasmids containing GFP-FTH into HBE cells and monitored the level of ectopically expressed GFP-FTH. The results showed that HDM induced the degradation of GFP-FTH, which could be prevented by autophagy inhibitor CQ (Figure 7N). Furthermore, we tested the protein levels of TFR, FPN1 and FTH in a time-course experiment and showed that FTH degradation is the major cause of iron-overload overwhelming iron-uptake/transport (Figure S3A). These data indicated that HDM induced NCOA4-mediated autophagic-dependent degradation of FTH, which was critical for the HDM-induced ferroptotic death of HBE cells (Figure 8).

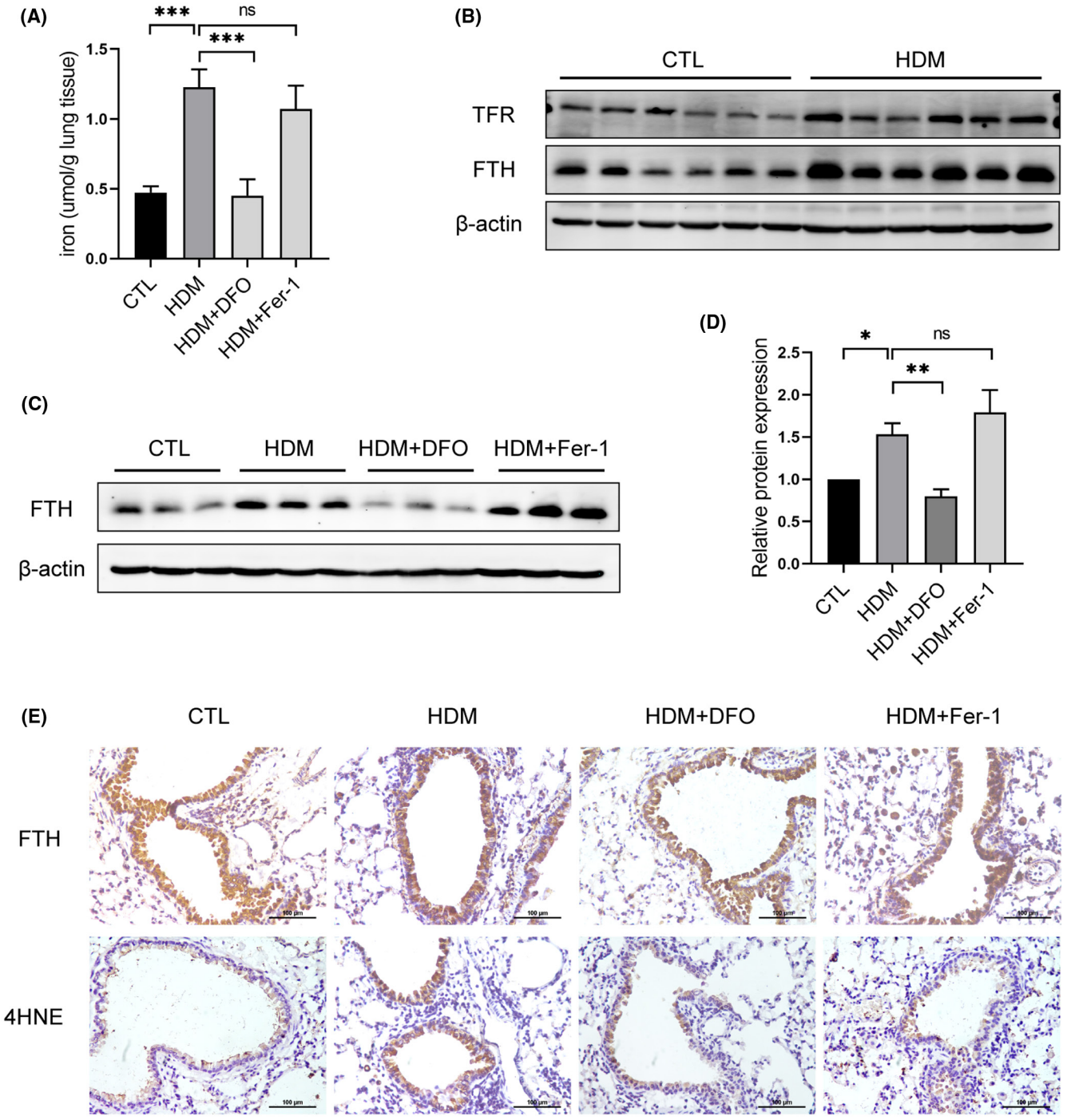

FIGURE 5 (A) The amount of free iron in mice lung tissue was measured by Iron Assay Kit. (B) Western blots analysis of FTH and TFR in mice lung tissue. (C,D) Western blots analysis of FTH in mouse lung tissue from these four groups and quantification of FTH protein levels relative to β-actin is shown (mean ± SEM, $n = 6$). (E) The expression of 4HNE and FTH in mouse lung airway were determined by immunohistochemical staining. Scale bar = 100 μm. The data are analyzed by one-way ANOVA with Dunnett's multiple comparison test. $^{*}p < .05$, $^{**}p < .01$, $^{***}p < .001$.

4 | DISCUSSION

In this study, we demonstrated that HDM induced ferroptosis of airway epithelial cells by activating NCOA4-mediated ferritinophagy. The degradation of ferritin further released large quantities of free iron produced via Fenton reactions and aggravated oxidative stress, lipid peroxidation and the release of cytokines and chemokines, such as IL-33, HMGB1, and TNF-α, which promote the inflammatory reactions in asthma.

The death of airway epithelial cells has been shown to play an important role in asthma pathogenesis.[31] Dead

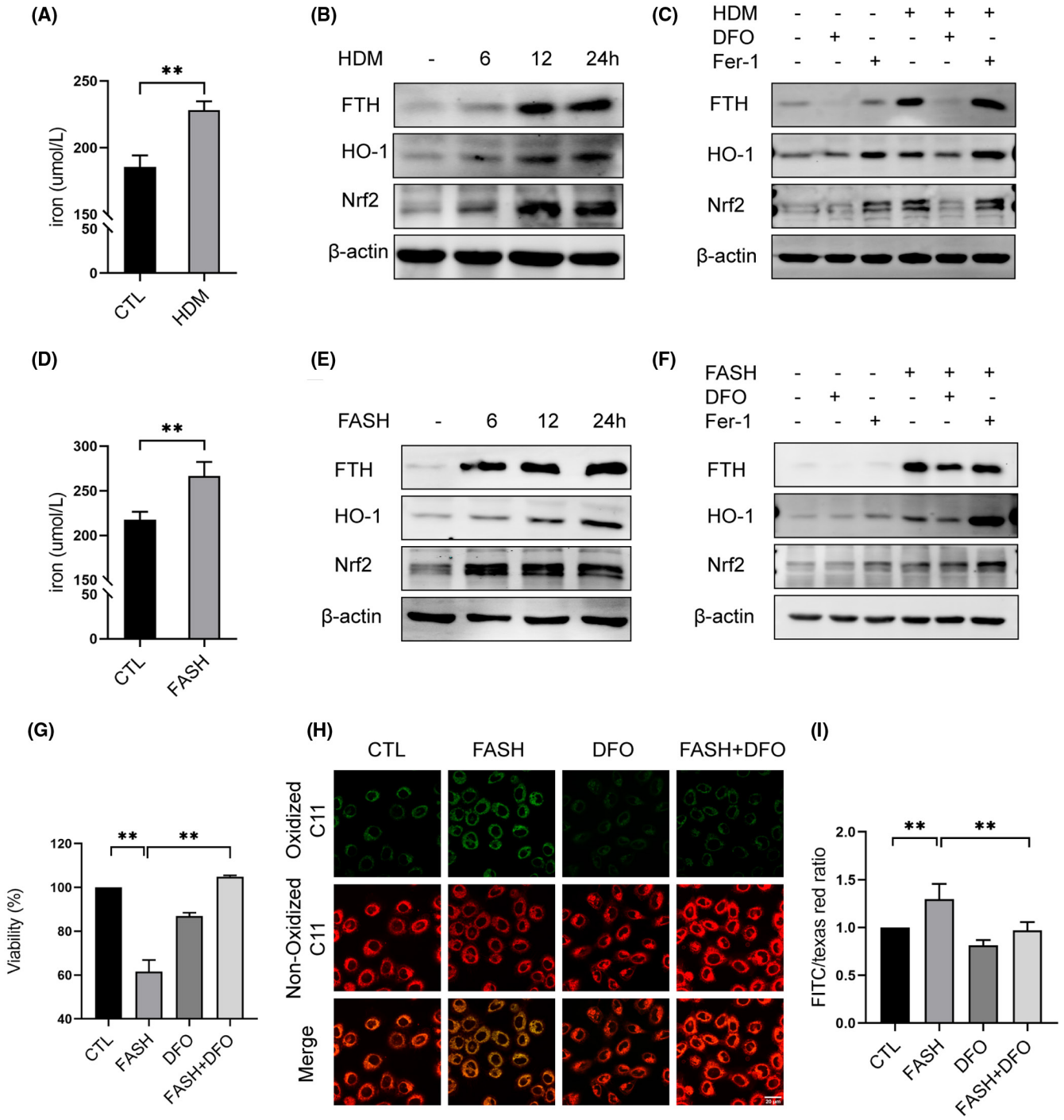

FIGURE 6 (A,D) The amount of free iron in cells treated with house dust mite (HDM) (800 μ/ml) or FASH (100 μM) was measured by Iron Colorimetric Assay Kit (student's *t*-test, $n = 3$). (B,E) Western blots analysis of FTH, HO-1 and Nrf2 in cells treated with HDM or FASH for 6, 12 and 24 h. (C,F) HBE cells were treated with HDM or FASH for 24 h. deferoxamine (50 μM) or ferrostatin-1 (20 μM) was added to HBE cells 1 h before HDM treatment. Western blots analysis of FTH, HO-1 and Nrf2 in cells. (G) Cell viability was assessed by CCK8 assay. (H,I) Lipid peroxidation was assessed by C11 BODIPY staining, and quantitative analysis of fluorescence intensity of each group. Scale bar = 20 μm. *$p < .05$, **$p < .01$, analyzed by one-way ANOVA with Dunnett's multiple comparison test, $n = 3$. All the data are presented as the mean ± SD.

epithelial cells are found in the airways of patients, but it remains to be determined whether these cells die via necroptosis, apoptosis or other types of cell death. It has been previously demonstrated that corticosteroids induce apoptosis of airway epithelial cells in asthma.[32] Toluene diisocyanate (TDI), a material in many kinds of industrial and consumer products, has been recognized as the most common cause of occupational asthma and found to induce pyroptosis of

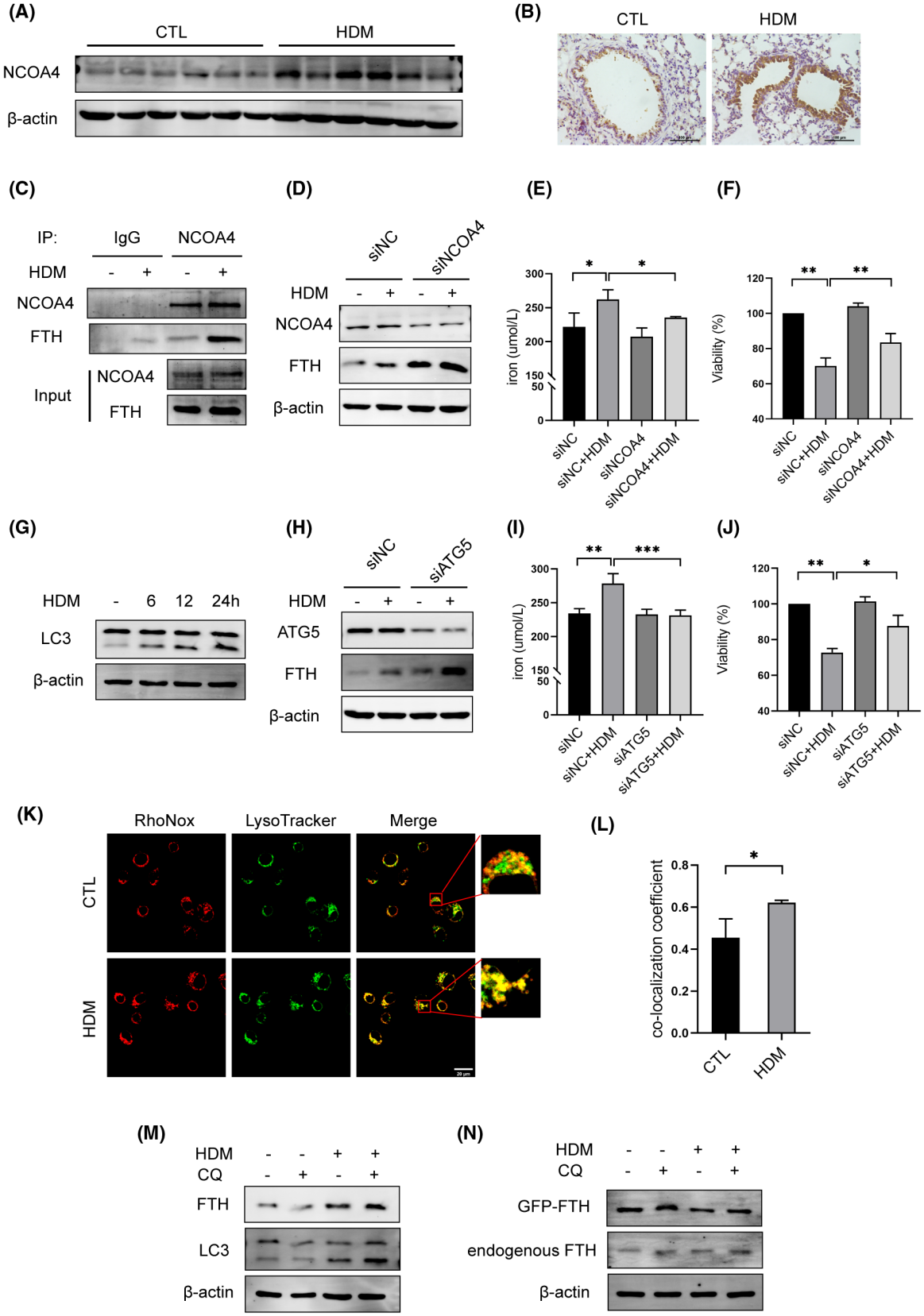

a human bronchial epithelial cells and bronchial epithelial cells of TDI-induced asthmatic mice.[33] However, exposure to HDM allergens is a major risk factor for allergic sensitization and asthma development,[34,35] and between 50% and 85% of asthmatic patients are allergic to HDMs.[36,37] Because they are among the most problematic allergens, HDMs in allergic asthma induction were the focus of our study. However, neither ZVAD-FMK, an apoptosis inhibitor, nor Nec-1, a

FIGURE 7 (A) Western blots analysis of NCOA4 in mouse lung tissue. (B) Immunohistochemical staining of NCOA4 in mouse lung airway. Scale bar = 100 μm. (C) Co-immunoprecipitation assays with NCOA4 and FTH. Samples before (Input) and after (IP) immunopurification were analyzed by immunoblotting using NCOA4 and FTH antibodies. (D–F) HBE cells were transfected with control short interfering RNA (siRNA) or NCOA4 siRNA for 48 h before house dust mite (HDM) (800 μ/ml) exposure. (D) Western blots showing expression levels of FTH and NCOA4 in HBE cells treated with HDM for 24 h. (E) Labile iron pool was measured in control or HDM treated HBE cells. (F) Cell viability was assessed by CCK8 assay. (G) Western blots showing expression levels of LC3 in HBE cells treated with HDM for 6, 12 and 24 h. (H–J) HBE cells were transfected with control siRNA or ATG5 siRNA for 48 h before HDM (800 μ/ml) exposure. (H) Western blots showing expression levels of FTH and ATG5 in HBE cells treated with HDM for 24 h. (I) Labile iron pool and (J) cell viability was measured. (K,L) RhoNox is a probe to detect ferrous, and LysoTracker Green DND-26 is a probe to detect lysosomes. The cells were stained for 30 min/37°C with RhoNox (red; 1 μM) and LysoTracker Green DND-26 (green; 100 nM). The yellow punctate staining demonstrates the electronic merge (Merge) of LysoTracker and RhoNox. Confocal microscopy analysis of co-localization of two probes. Scale bars = 20 μm. (M) Western blots analysis of FTH and LC3 expression level in HBE cells following HDM treatment with or without CQ (20 μM) 24 h. (N) HBE cells were treated as indicated. Western blots analysis of FTH and GFP-FTH expression level in cells. The data are presented as the mean ± SD, analyzed by one-way anova with Dunnett's multiple comparison test, $^{*}p < .05$, $^{**}p < .01$.

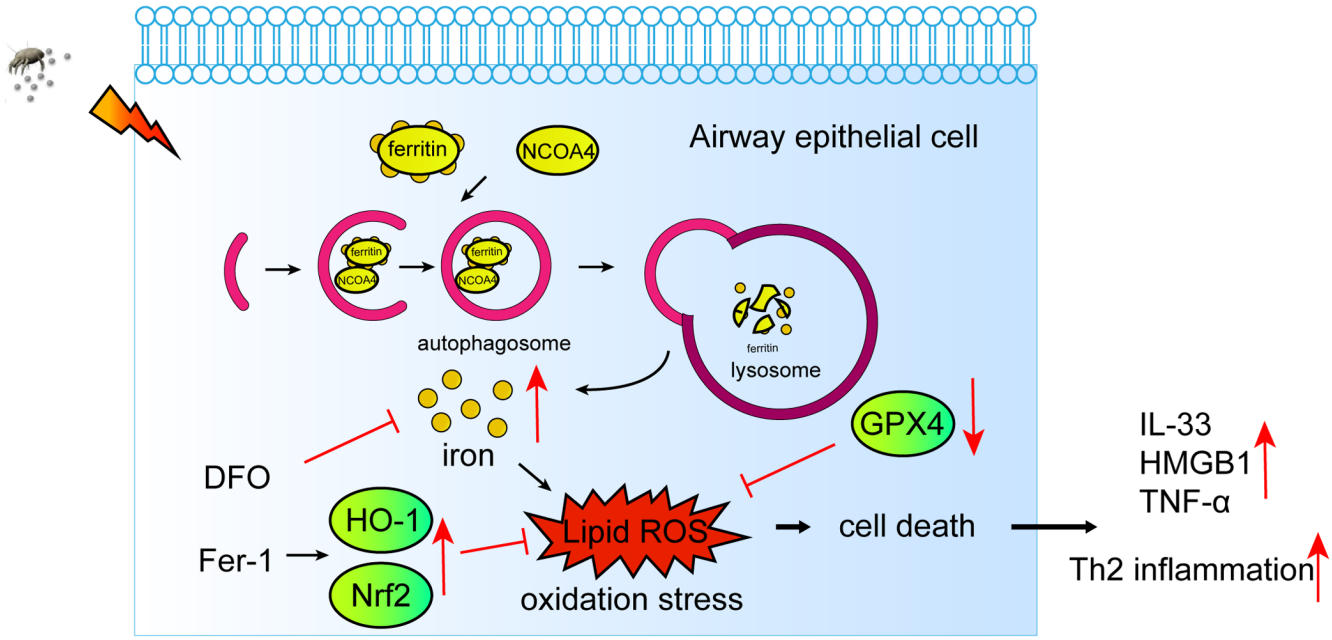

FIGURE 8 Schematic diagram of the molecular mechanisms underlying the house dust mite induce airway epithelial cell ferroptosis and promote inflammation by activating ferritinophagy in asthma.

necroptosis inhibitor, showed apparent inhibition of HDM-induced HBE cell death under our in vitro experimental conditions. Different doses of HDM extract may elicit different types of cell death at different time points; therefore, it is inappropriate to suggest that on type of death was predominant, and it is possible that asthmatic airway epithelial cells undergo different types of cell death. However, in this study, we showed that HDM-induced cell death is at least partially attributable to the ferroptosis of HBE cells. Our findings showed that HDMs also activated epithelial cells to release cytokines such as TNF-α, a representative necroptosis trigger, suggesting that ferroptosis might trigger other types of necrotic regulated cell death. This outcome may explain the reason that asthmatic airway epithelial cells may succumb to various types of death.

In our experiments, we found that there were higher levels of iron in the lung tissues of the asthma model. It has been reported that free iron levels or the expression of ferritin are related to asthma.[26,38,39] However, it is unclear whether altered iron levels play a role in the pathogenesis of asthma or whether these changes are a consequence of asthma pathogenesis. In our in vivo experiment, we found that DFO reduced the iron level in the lung and attenuated key features of asthma, including airway inflammation and T2 cytokine production. In our study, DFO, but not Fer-1, decreased HDM-induced upregulation of FTH (Figure 6C). DFO plays a role in binding free iron to inhibit ferroptosis, so it can bind with HDM-induced iron. As we mentioned above, the expression of FTH can be promoted by excess

iron. Thus, there is no need for cells to produce more FTH. However, the major function of Fer-1 is to inhibit lipid peroxidation, but not directly affect the expression of FTH. So, upregulation of FTH upon HDM treatment could be reversed by DFO but not Fer-1. Together, these data provide strong evidence that increased iron levels in tissue play key functional roles in the pathogenesis and increased severity of asthma.

Autophagy is the major intracellular degradation system by which cytoplasmic materials are degraded in lysosomes to maintain cell viability and homeostasis. The impairment or activation of autophagy contributes to the pathogenesis of diverse diseases, from neurodegenerative diseases to inflammatory disorders.[40] It has been reported that autophagy is involved in the execution of ferroptosis.[41] Importantly, lysosomal dysfunction and impaired autophagic flux are involved in the molecular pathogenesis of iron overload and lipotoxicity.[42,43] In the pathogenesis of asthma, autophagy has been shown to promote the epithelial Th2 response,[44,45] and autophagy inhibition in a murine model of asthma reduces airway responsiveness, eosinophilia, and inflammation.[46] Ferritinophagy has been identified as the novel selective autophagic degradation of ferritin mediated by the specific adaptor protein NCOA4.[28] Our experiments showed that NCOA4 knockdown significantly reduced the level of free iron and reestablished cell viability in response to HDM exposure, and excess iron promoted lipid peroxidation, further supporting the notion that free iron release by NCOA4-mediated ferritinophagy plays a regulatory role in ferroptosis. And our experimental results also showed that the use of CQ can reduce the expression of TNF-α, IL33 and HMGB1 in HDM-treated cells (Figure S4A–C). This mechanism may explain the relationship between asthma and autophagy and the reason that blockade of autophagy reduces airway inflammation in asthma.

As a kind of RCD, ferroptosis has positive effects on inflammation that have been confirmed by compelling evidence, and some ferroptosis inhibitors have been shown to exert anti-inflammatory activity in experimental models of certain diseases.[8] Type 2 inflammation is an important disease mechanism in a large subgroup of individuals with asthma, and type 2 cytokines provided multiple potential therapeutic targets for asthma.[47] A recent study has shown that environmental allergens house dust mite-induced asthma is associated with ferroptosis in the lungs, and the effect of agonists and inhibitors of ferroptosis on airway inflammation in HDM-induced asthma also requires further study.[48] In our in vivo experiment, we found that HDM-induced mice treated with ferroptosis inhibitors (DFO and Fer-1) had decreased IL-4, IL-5 and IL-13 expression levels. The results indicated that inhibition of ferroptosis reduced type 2 airway inflammation in asthma.

In conclusion, our findings support the likely role of ferritinophagy-mediated ferritin degradation during ferroptosis in asthma pathogenesis. The accumulation of free iron accelerates the inflammatory response during HDM exposure of airway epithelial cells, and DFO and Fer-1 treatment can relieve airway inflammation in HDM-induced asthma. Therefore, we believe that this study provides important clues for developing novel asthma treatments targeting ferroptosis by regulating iron hemostasis and lipid peroxidation. The extent to which ferroptosis is involved in asthma caused by different hazard factors remains largely unknown. The general areas needing clarification, such as the relationship between ferroptosis and iron, lipid peroxidation, oxidative stress injury, and autophagy need to be specifically addressed in lung diseases. More comprehensive and in-depth research on ferroptosis in the field of lung diseases is needed to expand our knowledge and techniques against lung impairment to increase the clinical beneficial outcomes in the future.

AUTHOR CONTRIBUTIONS

Zhaojin Zeng, Hangming Dong and Shaoxi Cai designed research experiments; Zhaojin Zeng and Haohua Huang performed experiments; Ye Lu, Wenshan Zhong, Weimou Chen, Ye Lu and Yujie Qiao collected and analyzed data; Xiaojing Meng and Fei Zou provided technical and material support; Jinming Zhang, Hangming Dong, Shaoxi Cai and Haijin Zhao prepared and edited the manuscript. All authors have given approval to the final version of the manuscript.

ACKNOWLEDGMENTS

We thank our colleagues et al. (Chronic Airways Diseases Laboratory, Department of Respiratory and Critical Care Medicine, Nanfang Hospital, Southern Medical University, Guangzhou, China,) for their generous support throughout this work.

FUNDING INFORMATION

This study was supported by the National Natural Science Foundation of China (81870058, 81970032, 82170032), the Natural Science Foundation of Guangdong Province (2017A030313849).

DISCLOSURES

The authors declare that they have no conflict of interest.

DATA AVAILABILITY STATEMENT

The datasets presented in this study can be found in the article/supplementary material.

ORCID

Shaoxi Cai https://orcid.org/0000-0003-2816-8262
Hangming Dong https://orcid.org/0000-0002-4476-9829

REFERENCES

1. Georas SN, Rezaee F. Epithelial barrier function: at the front line of asthma immunology and allergic airway inflammation. *J Allergy Clin Immunol*. 2014;134(3):509-520.
2. Sleiman PM, Flory J, Imielinski M, et al. Variants of DENND1B associated with asthma in children. *N Engl J Med*. 2010;362(1):36-44.
3. Lambrecht BN, Hammad H. Allergens and the airway epithelium response: gateway to allergic sensitization. *J Allergy Clin Immunol*. 2014;134(3):499-507.
4. Papi A, Brightling C, Pedersen SE, Reddel HK. Asthma. *Lancet*. 2018;391(10122):783-800.
5. Holgate ST, Roberts G, Arshad HS, Howarth PH, Davies DE. The role of the airway epithelium and its interaction with environmental factors in asthma pathogenesis. *Proc Am Thorac Soc*. 2009;6(8):655-659.
6. Lee KS, Jin SM, Kim HJ, Lee YC. Matrix metalloproteinase inhibitor regulates inflammatory cell migration by reducing ICAM-1 and VCAM-1 expression in a murine model of toluene diisocyanate-induced asthma. *J Allergy Clin Immunol*. 2003;111(6):1278-1284.
7. Dixon S, Lemberg K, Lamprecht M, et al. Ferroptosis: an iron-dependent form of nonapoptotic cell death. *Cell*. 2012;149(5):1060-1072.
8. Sun Y, Chen P, Zhai B, et al. The emerging role of ferroptosis in inflammation. *Biomed Pharmacother*. 2020;127:110108.
9. Friedmann Angeli JP, Schneider M, Proneth B, et al. Inactivation of the ferroptosis regulator Gpx4 triggers acute renal failure in mice. *Nat Cell Biol*. 2014;16(12):1180-1191.
10. Imai H, Hirao F, Sakamoto T, et al. Early embryonic lethality caused by targeted disruption of the mouse PHGPx gene. *Biochem Biophys Res Commun*. 2003;305(2):278-286.
11. Skouta R, Dixon SJ, Wang J, et al. Ferrostatins inhibit oxidative lipid damage and cell death in diverse disease models. *J Am Chem Soc*. 2014;136(12):4551-4556.
12. Chen Y, Zhang P, Chen W, Chen G. Ferroptosis mediated DSS-induced ulcerative colitis associated with Nrf2/HO-1 signaling pathway. *Immunol Lett*. 2020;225:9-15.
13. Xu M, Tao J, Yang Y, et al. Ferroptosis involves in intestinal epithelial cell death in ulcerative colitis. *Cell Death Dis*. 2020;11(2):86.
14. Li Y, Feng D, Wang Z, et al. Ischemia-induced ACSL4 activation contributes to ferroptosis-mediated tissue injury in intestinal ischemia/reperfusion. *Cell Death Differ*. 2019;26(11):2284-2299.
15. Song Y, Yang H, Lin R, Jiang K, Wang BM. The role of ferroptosis in digestive system cancer. *Oncol Lett*. 2019;18(3):2159-2164.
16. Hu Z, Zhang H, Yi B, et al. VDR activation attenuate cisplatin induced AKI by inhibiting ferroptosis. *Cell Death Dis*. 2020;11(1):73.
17. Chen C, Wang D, Yu Y, et al. Legumain promotes tubular ferroptosis by facilitating chaperone-mediated autophagy of GPX4 in AKI. *Cell Death Dis*. 2021;12(1):65.
18. Martin-Sanchez D, Ruiz-Andres O, Poveda J, et al. Ferroptosis, but not necroptosis, is important in nephrotoxic folic acid-induced AKI. *J Am Soc Nephrol*. 2017;28(1):218-229.
19. Li Y, Cao Y, Xiao J, et al. Inhibitor of apoptosis-stimulating protein of p53 inhibits ferroptosis and alleviates intestinal ischemia/reperfusion-induced acute lung injury. *Cell Death Differ*. 2020;27(9):2635-2650.
20. Yang Y, Tai W, Lu N, et al. lncRNA ZFAS1 promotes lung fibroblast-to-myofibroblast transition and ferroptosis via functioning as a ceRNA through miR-150-5p/SLC38A1 axis. *Aging*. 2020;12(10):9085-9102.
21. Yoshida M, Minagawa S, Araya J, et al. Involvement of cigarette smoke-induced epithelial cell ferroptosis in COPD pathogenesis. *Nat Commun*. 2019;10:3145.
22. Wenzel SE, Tyurina YY, Zhao J, et al. PEBP1 wardens ferroptosis by enabling lipoxygenase generation of lipid death signals. *Cell*. 2017;171(3):628-641.e26.
23. Zhao J, Dar HH, Deng Y, et al. PEBP1 acts as a rheostat between prosurvival autophagy and ferroptotic death in asthmatic epithelial cells. *Proc Natl Acad Sci USA*. 2020;117(25):14376-14385.
24. Wood LG, Gibson PG, Garg ML. Biomarkers of lipid peroxidation, airway inflammation and asthma. *Eur Respir J*. 2003;21(1):177-186.
25. Sharma A, Bansal S, Nagpal RK. Lipid peroxidation in bronchial asthma. *Indian J Pediatr*. 2003;70(9):715-717.
26. Ali MK, Kim RY, Brown AC, et al. Crucial role for lung iron level and regulation in the pathogenesis and severity of asthma. *Eur Respir J*. 2020;55(4):1901340.
27. Bibi H, Vinokur V, Waisman D, et al. Zn/Ga-DFO iron-chelating complex attenuates the inflammatory process in a mouse model of asthma. *Redox Biol*. 2014;2:814-819.
28. Mancias JD, Wang X, Gygi SP, Harper JW, Kimmelman AC. Quantitative proteomics identifies NCOA4 as the cargo receptor mediating ferritinophagy. *Nature*. 2014;509(7498):105-109.
29. Gao MH, Monian P, Pan QH, Zhang W, Xiang J, Jiang XJ. Ferroptosis is an autophagic cell death process. *Cell Res*. 2016;26(9):1021-1032.
30. Liu MX, Shan MT, Zhang YX, Guo ZL. Progranulin protects against airway remodeling through the modulation of autophagy via HMGB1 suppression in house dust mite-induced chronic asthma. *J Inflamm Res*. 2021;14:3891-3904.
31. Lambrecht BN, Hammad H. Death at the airway epithelium in asthma. *Cell Res*. 2013;23(5):588-589.
32. Dorscheid DR, Wojcik KR, Sun S, Marroquin B, White SR. Apoptosis of airway epithelial cells induced by corticosteroids. *Am J Respir Crit Care Med*. 2001;164(10 Pt 1):1939-1947.
33. Zhuang J, Cui H, Zhuang L, et al. Bronchial epithelial pyroptosis promotes airway inflammation in a murine model of toluene diisocyanate-induced asthma. *Biomed Pharmacother*. 2020;125:109925.
34. Arbes SJ, Cohn RD, Yin M, et al. House dust mite allergen in US beds: results from the first national survey of lead and allergens in housing. *J Allergy Clin Immunol*. 2003;111(2):408-414.
35. Hales BJ, Martin AC, Pearce LJ, et al. IgE and IgG anti-house dust mite specificities in allergic disease. *J Allergy Clin Immunol*. 2006;118(2):361-367.
36. Thomas WR, Smith WA, Hales BJ, Mills KL, O'Brien RM. Characterization and immunobiology of house dust mite allergens. *Int Arch Allergy Immunol*. 2002;129(1):1-18.
37. Gregory LG, Lloyd CM. Orchestrating house dust mite-associated allergy in the lung. *Trends Immunol*. 2011;32(9):402-411.
38. Hur G-Y, Choi G-S, Sheen S-S, et al. Serum ferritin and transferrin levels as serologic markers of methylene diphenyl

diisocyanate-induced occupational asthma. *J Allergy Clin Immun*. 2008;122(4):774-780.
39. Palikhe NS, Kim JH, Park HS. Biomarkers predicting isocyanate-induced asthma. *Allergy Asthma Immun*. 2011;3(1):21-26.
40. Mizushima N, Komatsu M. Autophagy: renovation of cells and tissues. *Cell*. 2011;147(4):728-741.
41. Zhou BR, Liu J, Kang R, Klionsky DJ, Kroemer G, Tang DL. Ferroptosis is a type of autophagy-dependent cell death. *Semin Cancer Biol*. 2020;66:89-100.
42. Du J, Zhu W, Yang LI, et al. Reduction of polyethylenimine-coated iron oxide nanoparticles induced autophagy and cytotoxicity by lactosylation. *Regen Biomater*. 2016;3(4):223-229.
43. Khan MI, Mohammad A, Patil G, Naqvi SAH, Chauhan LKS, Ahmad I. Induction of ROS, mitochondrial damage and autophagy in lung epithelial cancer cells by iron oxide nanoparticles. *Biomaterials*. 2012;33(5):1477-1488.
44. Dickinson JD, Alevy Y, Malvin NP, et al. IL13 activates autophagy to regulate secretion in airway epithelial cells. *Autophagy*. 2016;12(2):397-409.
45. Poon A, Eidelman D, Laprise C, Hamid Q. ATG5, autophagy and lung function in asthma. *Autophagy*. 2012;8(4):694-695.
46. Liu JN, Suh DH, Trinh HKT, Chwae YJ, Park HS, Shin YS. The role of autophagy in allergic inflammation: a new target for severe asthma. *Exp Mol Med*. 2016;48(7):e243.
47. Fahy JV. Type 2 inflammation in asthma - present in most, absent in many. *Nat Rev Immunol*. 2015;15(1):57-65.
48. Tang WF, Dong M, Teng FZ, et al. Environmental allergens house dust mite-induced asthma is associated with ferroptosis in the lungs. *Exp Ther Med*. 2021;22(6):1483.

SUPPORTING INFORMATION

Additional supporting information may be found in the online version of the article at the publisher's website.

How to cite this article: Zeng Z, Huang H, Zhang J, et al. HDM induce airway epithelial cell ferroptosis and promote inflammation by activating ferritinophagy in asthma. *FASEB J*. 2022;36:e22359. doi:10.1096/fj.202101977RR

Supplementary Figure1

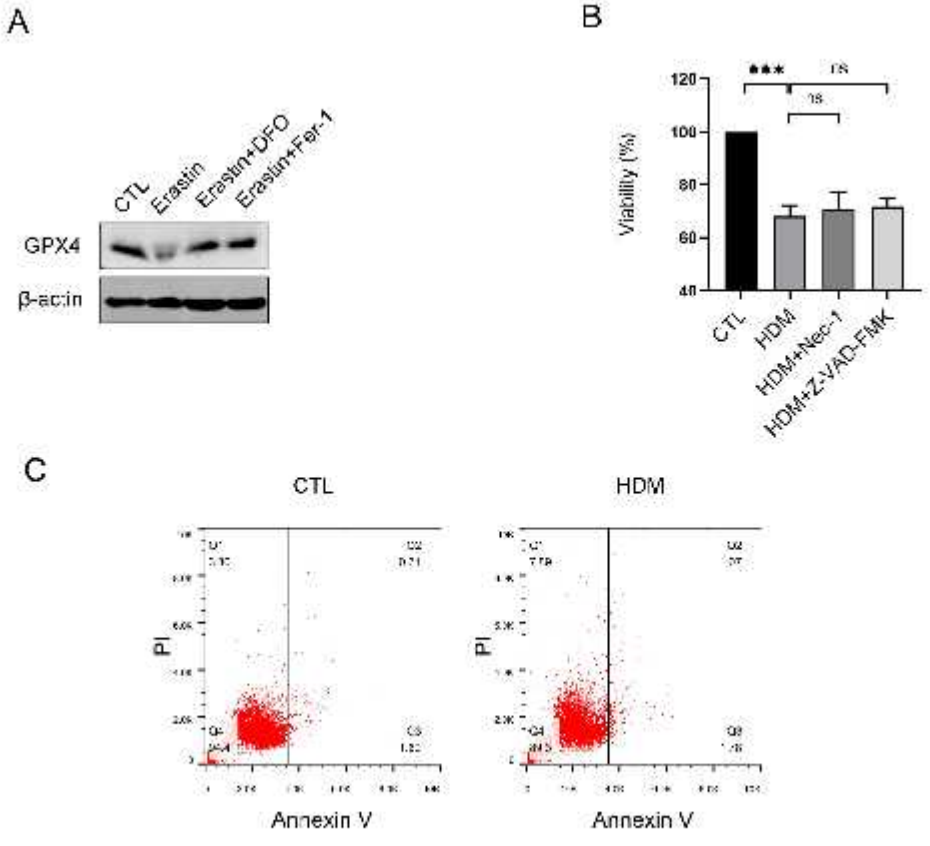

Supplementary Figure2

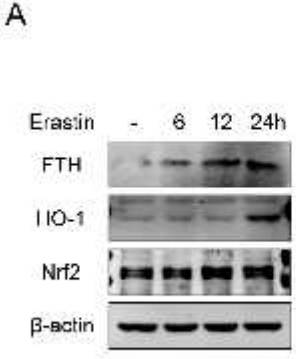

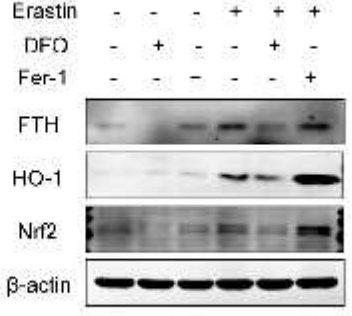

Supplementary Figure3

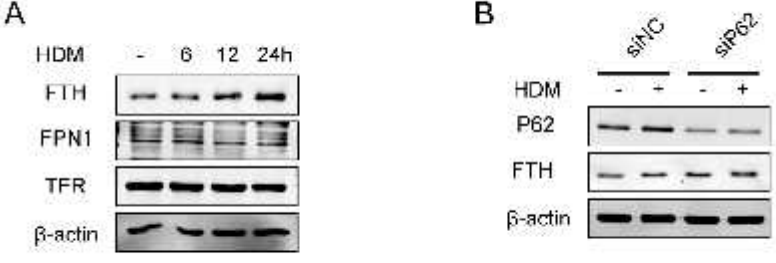
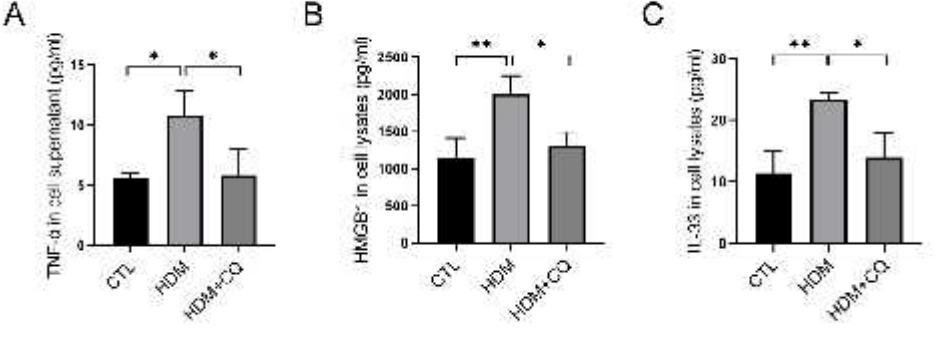
Supplementary Figure4